Available online at www.sciencedirect.com
ScienceDirect
Polymer 47 (2006) 6524–6535
polymer
www.elsevier.com/locate/polymer

# Supramolecular assemblies of amphiphilic PMMA-*block*-PAA stars in aqueous solutions

Satu Strandman [a], Sami Hietala [a], Vladimir Aseyev [a], Benita Koli [b], Sarah J. Butcher [b], Heikki Tenhu [a,*]

[a] *Laboratory of Polymer Chemistry, University of Helsinki, P.O. Box 55, FIN-00014 HY, Helsinki, Finland*
[b] *Institute of Biotechnology and Department of Biological and Environmental Sciences, University of Helsinki, P.O. Box 65, FIN-00014 HY, Helsinki, Finland*

Received 19 May 2006; received in revised form 18 July 2006; accepted 23 July 2006

**Abstract**

Self-assembling properties of an amphiphilic star block copolymer, 4-arm (PMMA-*b*-PAA)$_4$ with poly(methyl methacrylate) core and poly(acrylic acid) shell, have been investigated in aqueous solutions. The stars have been observed to aggregate in a complex manner in aqueous solutions, depending on the presence or absence of salt. Screening of the electrostatic repulsion between the polyelectrolyte blocks by adding salt triggers the formation of worm-like micelles. The presence of worm-like micelles in saline solutions was revealed by Kratky analysis of the light scattering data. The coexistence of different micellar morphologies was visualized by direct imaging by cryoTEM. Due to the balance between the electrostatic and hydrophobic interactions semidilute solutions show interesting rheological properties. Shear thinning behavior of salt-free solutions and their time-dependent gelation have been observed, thus indicating the strong tendency of the polymers to aggregate.


*Keywords:* Amphiphilic star block copolymers; Self-assembling; Micellization

## 1. Introduction

The self-assembling of amphiphilic block copolymers in solution provides an intriguing way to produce nanostructures with versatile compositions and various morphologies resembling those observed in nature. The most common of these supramolecular assemblies are not only spherical micelles, worm micelles, and vesicles [1–3], but also more complex morphologies can be obtained, such as multicompartment micelles [4], toroids [5], and helices [6]. As solvent plays an important role in the formation of noncovalent assemblies [7], changing the solvent composition, ionic strength or pH can induce the self-assembling of block copolymers or trigger the transition between the assembled geometries [3,8–10]. It is essential to know the factors that influence the formation of nanostructures, as precise control over the morphology of the aggregates is required for the potential applications, such as targeted drug delivery [11], nanolithography [12] and nanoreactors [13]. Hence, studying the kinetics and mechanisms of self-assembly [14,15], and trapping the morphologies by cross-linking [16–18] have attracted much interest during recent years.

In addition to associated linear block copolymers, aqueous colloidally stable dispersions can be obtained, for instance, from spherical polymer brushes prepared by fixing hydrophilic polymers on the surface of particles or dendrimers [19] or by synthesizing amphiphilic star polymers [20]. The soft soluble outer layer contributes significantly to the overall behavior of the brushes. A number of different polymer systems representing this class of 'soft colloids' have been studied with respect to their structural and dynamic properties [21–28]. The softness of a colloidal system is described

* Corresponding author. Tel.: +358 9 19150334; fax: +358 9 19150330.
*E-mail address:* heikki.tenhu@helsinki.fi (H. Tenhu).

0032-3861/$ - see front matter © 2006 Elsevier Ltd. All rights reserved.
doi:10.1016/j.polymer.2006.07.057

through the repulsive interactions between the objects (particles, micelles, polymer brushes, etc.) and varies from extremely soft linear polymer chains to nonoverlapping hard spheres [25,29]. The softer the objects are, the more they can interpenetrate and the more they can be compressed [25]. Spherical polymer brushes represent a system of intermediate softness, which can be controlled by adjusting the ratio of the thickness of the stabilizing layer to the core or by adjusting the degree of grafting (number of arms in a star polymer) [25,29]. The way these molecules further self-assemble influences their viscoelastic properties and thus their applicability, for example, in surface coatings and as rheological control agents and stabilizers.

Amphiphilic star block copolymers may exist in dilute aqueous solutions as single molecules, 'unimolecular micelles', and in this state the dimensions of individual stars as well as the dynamics of the blocks can be investigated [30,31]. Additionally, if the corona of the star polymer is composed of a polyelectrolyte, it is likely to respond to changes in the solvent salinity or pH. The micellar structures of block copolymers can be changed by a careful transfer from the solvent preferred by one block to the solvent preferred by the other [1]. As star block copolymers have fixed configurations, transfer to the solvent preferred by the inner block may lead to the precipitation of the polymers already at relatively low concentrations, while in solvents preferred by the outer block colloidally stable solutions may be obtained in a wide concentration range. Nevertheless, the solubility is ultimately dependent on the ratio of the block lengths [30,31]. In the case of amphiphilic stars where the core is hydrophobic and the shell hydrophilic, the core typically is in a solid-like state in water, resembling a hard colloidal sphere in solution. The solubilized corona of the molecule gives a polymer-like behavior to the particles. Several research groups have reported the aggregation of amphiphilic star polymers in aqueous solutions [32–35], and miktoarm stars with both hydrophobic and hydrophilic arms have been observed to form cylindrical and multicompartment micelles in solution [4,36].

In this paper we describe the self-assembling of an amphiphilic star block copolymer, 4-arm (PMMA-*b*-PAA)$_4$ with poly(methyl methacrylate) inner blocks and poly(acrylic acid) outer blocks in aqueous solutions. The (PMMA-*b*-PAA)$_4$ star was dissolved directly in water, and no organic solvents or dialysis was required. Light scattering was used to investigate the polymer in saline solutions and the data were analyzed using Kratky representation, revealing the presence of nonspherical aggregates. Concentration dependence of viscoelastic properties of the solutions was examined in order to explore the dynamics of the stars in the absence of salt. Direct imaging by cryo-transmission electron microscopy (cryoTEM) was utilized to visualize the morphologies of micelle-like aggregates, which showed the coexistence of both spherical and worm-like micelles in saline solutions. The association of the star-like macromolecules resembles that of charged biopolymers, such as actin, since a balance between attractive and repulsive forces is required for the formation of cylindrical assemblies and can be manipulated by the ionic strength of the solvent [37].

## 2. Experimental section

### 2.1. Materials

*tert*-Butyl acrylate (Aldrich), diphenyl ether (Merck) and methyl methacrylate (Fluka) were dried with $CaCl_2$ or $CaH_2$ and distilled in vacuum, the last one after the addition of a small amount of hydroquinone. Trifluoroacetic acid (TFA, Fluka), CuBr (99.999%), 2,2′-bipyridyl, *N*,*N*,*N*′,*N*′,*N*″-pentamethyldiethylenetriamine (PMDETA) and ethylene carbonate (all from Aldrich) were used as received. CuCl (Merck) was purified as described by Nikitine et al. [38]. Dichloromethane (Fluka) was dried on molecular sieves. The synthesis of the multifunctional initiator, octa-2-bromoisobutyryltetraethylresorcinarene, has been described earlier [39].

### 2.2. Syntheses and characterization

#### 2.2.1. Synthesis of a star-like poly(methyl methacrylate) macroinitiator (PMMA)$_4$

The polymerization was carried out in a flask equipped with a high vacuum valve. The flask was charged with the initiator (224 mg, $1.25 \times 10^{-4}$ mol), 2,2′-bipyridyl (312 mg, 2.0 mmol), diphenyl ether (43 mL, 50% from the total volume of the reaction mixture) and methyl methacrylate (40.0 g, 42.8 mL, 0.40 mol). The solution was degassed by two freeze–thaw cycles under high vacuum, followed by the addition of CuCl (98.7 mg, 1.0 mmol) and three freeze–thaw cycles. The flask was placed in an oil bath thermostated at 90 °C. As the star polymerization of methyl methacrylate is prone to bimolecular coupling, the polymerization was terminated at low conversion (Table 1). After the reaction time of 13 min, during which the polymerization reached 13.1% conversion, the solution was cooled by dipping the flask into liquid nitrogen. The solution was brought to room temperature, after which the content was dissolved in THF and passed through a column packed with silica (4/5) and neutral alumina (1/5) in two layers to remove the copper salts. The polymer was precipitated in methanol and dried *in vacuo* at room temperature. The polymer was purified by dialysis in THF, precipitated and lyophilized. The multifunctional resorcinarene-based initiator in this polymerization produces star-like polymers with 4 arms at the studied reaction conditions due to steric hindrance, which has been discussed earlier [39,40]. Despite the low conversion, the presence of coupled stars was revealed by static light scattering in THF, which gave weight-average molar mass $M_w$ 88,800 g/mol while the $M_w$ determined by SEC was 40,500 g/mol. In our experience on parallel determination of molar masses by SEC and SLS, this large difference in molar masses does not stem from the calibration of SEC by linear standards. Nevertheless, the SEC trace given by the RI detector (Fig. 1) is nearly symmetrical, indicating a very low fraction of coupled stars.

$^1$H NMR (200 MHz, $CDCl_3$) $\delta$ ppm: 0.78, 0.95, 1.15, 1.32 and 1.39 (3H, $>C(CH_3)-$), 1.75 and 1.82 (2H, $-CH_2-$), 3.53 (3H, $-CH_3$), 3.70 (3H, $-CH_3$, endgroup). Molar mass $M_n$

Table 1
Characteristics of a star-like $(PMMA)_4$ homopolymer, the corresponding $(PMMA\text{-}b\text{-}ptBA)_4$ block copolymer, and the amphiphilic $(PMMA\text{-}b\text{-}PAA)_4$ star

| Polymer | Conv (%) | $M_n$ (theor) (g/mol) | $M_n$ (NMR)[c] (g/mol) | $M_n$ (SEC)[e] (g/mol) | PDI | $M_w$ (SEC) (g/mol) | $M_w$ (SLS) (g/mol) |
|---|---|---|---|---|---|---|---|
| $(PMMA)_4$ | 13.1 | 43,600[a] | 26,700 | 31,100 | 1.30 | 40,500 | 88,800[g] |
| $(PMMA\text{-}b\text{-}ptBA)_4$ | 19.8 | 112,400[b] | 90,200 | 102,600 | 1.33 | 137,700 | 400,000[h] |
| $(PMMA\text{-}b\text{-}PAA)_4$ | | | 61,300[d] | 71,200[f] | 1.33 | | |

[a] $M_n$ (theor) = [M]/[I] × conv × M(monomer) + M(initiator), where 'conv' is for conversion.
[b] $M_n$ (theor) = [M]/[I] × conv × M(monomer) + $M_n$ (SEC, macroinitiator).
[c] Estimated by $^1$H NMR analysis.
[d] Calculated from $M_n$ (NMR) of $(PMMA\text{-}b\text{-}ptBA)_4$ after the hydrolysis of *tert*-butyl ester groups.
[e] SEC determinations in THF using calibration by poly(methyl methacrylate) standards.
[f] Calculated from $M_n$ (SEC) of $(PMMA\text{-}b\text{-}ptBA)_4$ after the hydrolysis of *tert*-butyl ester groups.
[g] Determined by static light scattering in THF, d*n*/d*c* = 0.092 mL/g.
[h] Determined by static light scattering in toluene, d*n*/d*c* = −0.032 mL/g.

(NMR) was estimated by comparing the signal of the endgroup to the signals from $-CH_3$ groups.

$^{13}$C NMR (200 MHz, $CDCl_3$) $\delta$ ppm: 16.47 and 18.73 (1C, $>C(CH_3)-$), 44.82 (1C, $-CH_2-$), 51.79 (1C, $-OCH_3$), 54.37 (1C, $>C(CH_3)-$), 177.00 and 177.85 (1C, >C=O).

FT-IR (solid, ATR) cm$^{-1}$: 750 (w), 810 (w), 841 (w), 966 (w), 988 (m), 1062 (w), 1146 (s), 1191 (m), 1241 (m), 1269 (m), 1368 (w), 1388 (w), 1435 (m), 1483 (w), 1726 (s), 2950 (w), 2994 (w).

### 2.2.2. Synthesis of a star block copolymer $(PMMA\text{-}b\text{-}ptBA)_4$

The polymerization was carried out in a flask equipped with a high vacuum valve. The star-like poly(methyl methacrylate) macroinitiator (1.5 g, $4.8 \times 10^{-5}$ mol) with molar mass 31,100 g/mol and ethylene carbonate (3.31 g, 37.6 mmol, 16.8% from the mass of the monomer) were dissolved in *tert*-butyl acrylate (19.8 g, 0.15 mol, 22.6 mL). PMDETA (41.6 μL, 33.4 mg, 0.19 mmol) was added to the solution and the solution was degassed by two freeze–thaw cycles. CuBr (27.8 mg, 0.19 mmol) was added, followed by three freeze–thaw cycles. The solution was stirred at room temperature for 5 min before placing it in an oil bath thermostated at 90 °C. Acrylates have a lower tendency towards coupling side reactions than methacrylates [41] and hence, the polymerization was terminated at a slightly higher conversion (Table 1) than one of the macroinitiators. After the reaction time of 28 min, during which the polymerization reached 19.8% conversion, the solution was cooled by immersing the flask into liquid nitrogen. The solution was brought to room temperature, after which the content was dissolved in THF and passed twice through a column packed with silica (4/5) and neutral alumina (1/5) in two layers. The polymer was precipitated in a mixture of methanol and water (8:2), washed with water and lyophilized. According to SEC, the molar mass had increased during polymerization, but a part of the macroinitiator had not reacted, and therefore the polymer was purified by ultrafiltration in acetone using regenerated cellulose membrane (NMWL 100,000 g/mol, Millipore), followed by precipitation as above. During this procedure some of the block copolymer may have been lost. The unimodal and symmetrical SEC traces of the block copolymer after this procedure are shown in Fig. 1. The successful block copolymerization can also be confirmed from the disappearance of the signal from the endgroups of $(PMMA)_4$ at 3.70 ppm (Fig. 2a and b). The molar ratio of the blocks, determined by $^1$H NMR, is 1:2 (PMMA:ptBA), which is in accordance with the ratio estimated from the molar masses given by SEC. The composition of the block copolymer calculated from the ratio of the blocks and the value of $M_n$ (SEC) (Table 1) is $(PMMA_{73}\text{-}b\text{-}ptBA_{143})_4$. The $M_w$ of the purified block copolymer given by SEC in THF was 137,700 g/mol and the $M_w$ given by static light scattering in toluene was 400,000 g/mol (Table 1).

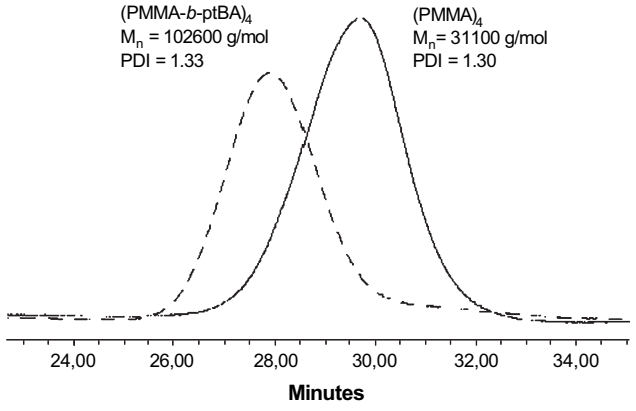


Fig. 1. SEC traces of star-like $(PMMA)_4$ macroinitiator and corresponding $(PMMA\text{-}b\text{-}ptBA)_4$ block copolymer.

The SEC instrument was calibrated using linear poly(methyl methacrylate) standards, which naturally causes experimental error in the molar mass results of the star-like block copolymer. The results given by static light scattering may also deviate from the actual molar mass because of the possible difference in the refractive index increments (d*n*/d*c*) of PMMA and ptBA blocks, or because of the presence of coupled block copolymer stars due to star–star coupling reactions during the synthesis. Moreover, contrast between the solvent and the star block copolymer was very low (the d*n*/d*c* of the star block copolymer in toluene was −0.0315 mL/g at $\lambda = 488$ nm).

$^1$H NMR (200 MHz, $CDCl_3$) $\delta$ ppm: 0.78, 0.95 and 1.06 (3H, $>C(CH_3)-$, PMMA), 1.37 (9H, $-C(CH_3)_3$, ptBA), 1.75 and 1.82 (4H, $-CH_2-$), 2.18 (1H, $-CH-$, ptBA), 3.53 (3H, $-CH_3$, PMMA). Molar mass $M_n$ (NMR) was estimated by using the block ratio and the $M_n$ (NMR) of $(PMMA)_4$.

$^{13}$C NMR (200 MHz, $CDCl_3$) $\delta$ ppm: 16.46 (1C, $>C(CH_3)-$, PMMA), 28.07 (3C, $-C(CH_3)_3$, ptBA), 35.88 (1C, $-CH-$,

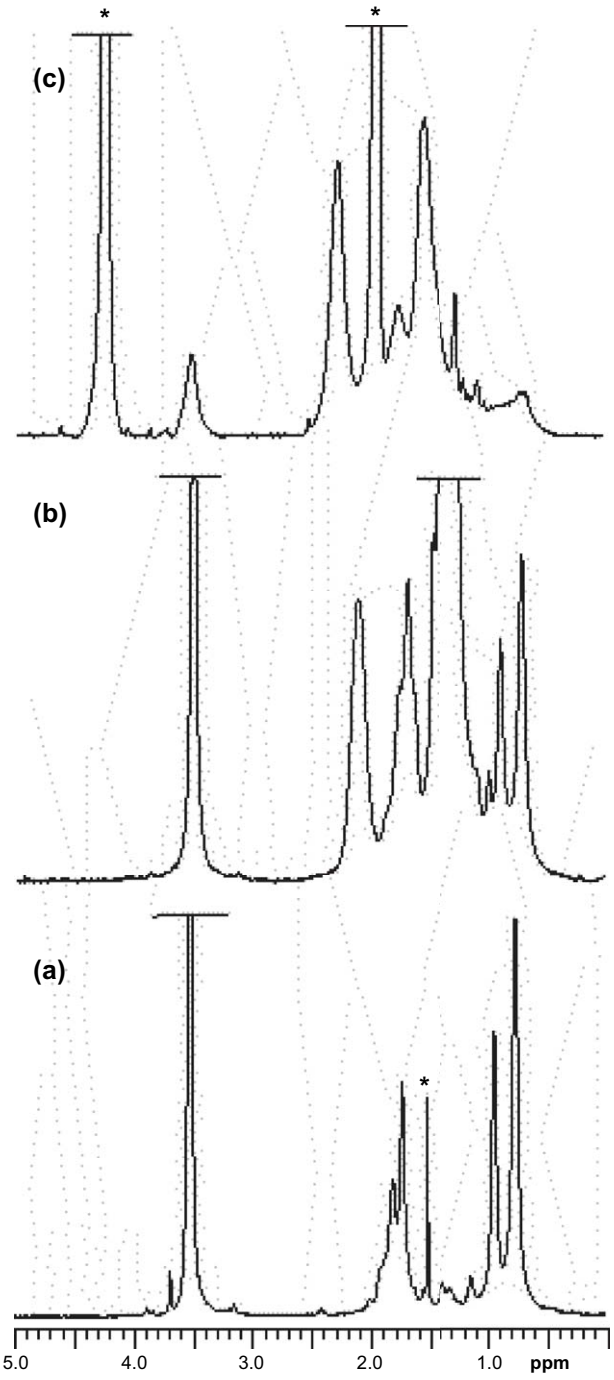


Fig. 2. $^1$H NMR spectra of the star-like polymers. Spectral assignments are listed in Section 2 where the most important signals for the characterization have been highlighted. (a) $(PMMA)_4$ in $CDCl_3$, (b) $(PMMA\text{-}b\text{-}ptBA)_4$ in $CDCl_3$, (c) $(PMMA\text{-}b\text{-}PAA)_4$ in acetone-$d_6$/$D_2O$. The signals from solvents have been marked by asterisks.

ptBA), 41.92 (1C, $-CH_2-$, ptBA), 44.56 (1C, $-CH_2-$, PMMA), 51.78 (1C, $-OCH_3$, PMMA), 54.36 (1C, $>C(CH_3)-$), PMMA), 80.33 (1C, $-C(CH_3)_3$, ptBA), 174.16 (1C, >C=O, ptBA), 176.96 and 177.80 (1C, >C=O, PMMA).

FT-IR (solid, ATR) cm$^{-1}$: 751 (w), 845 (m), 908 (w), 963 (w), 992 (w), 1035 (w), 1062 (w), 1144 (s), 1254 (m), 1335 (w), 1367 (m), 1393 (w), 1448 (w), 1480 (w), 1725 (s), 2935 (w), 2978 (w), 2997 (w).

### 2.2.3. Conversion of $(PMMA\text{-}b\text{-}ptBA)_4$ star block copolymer to amphiphilic $(PMMA\text{-}b\text{-}PAA)_4$

Hydrolysis with trifluoroacetic acid in dichloromethane described by Ma and Wooley [16] was used to yield star-like $(PMMA\text{-}b\text{-}PAA)_4$ (shown in Scheme 1). Block copolymer was dissolved in dry $CH_2Cl_2$. Trifluoroacetic acid (5 equiv to the *tert*-butyl ester) was added and the mixture was stirred at room temperature for 24 h. The course of the reaction was monitored by $^1$H NMR from the disappearance of the resonance signal from protons in *tert*-butyl ester at 1.37 ppm. The signal from the −CH− protons of poly(*tert*-butyl acrylate) at 2.18 ppm disappeared while that of poly(acrylic acid) appeared at 2.39 ppm upon hydrolysis. No cleavage of the methyl ester groups of poly(methyl methacrylate) was observed during the 24 h reaction time. The solution was concentrated by evaporation. The polymer was precipitated in diethyl ether and dried *in vacuo* at room temperature. $(PMMA\text{-}b\text{-}PAA)_4$ polymer was dialyzed in a water−acetone mixture (3:1), after which a part of the acetone was evaporated. The polymer was precipitated in diethyl ether, dissolved in water and dried *in vacuo* at room temperature. Since the dry polymer did not redissolve in pure water, it was dissolved in 0.01 M NaOH (aq) solution. Ion exchange resin (Dowex 50W, Fluka) was added to the solution, the mixture was stirred for 30 min and filtered. The polymer solution was dialyzed in water and lyophilized. The FT-IR spectrum of the dry amphiphile showed a broad band of −COOH at $\nu > 2400$ cm$^{-1}$ confirming the cleavage of *tert*-butyl functionalities. The selective cleavage changed the solubility of the star block copolymer significantly turning the polymer soluble in water and insoluble in

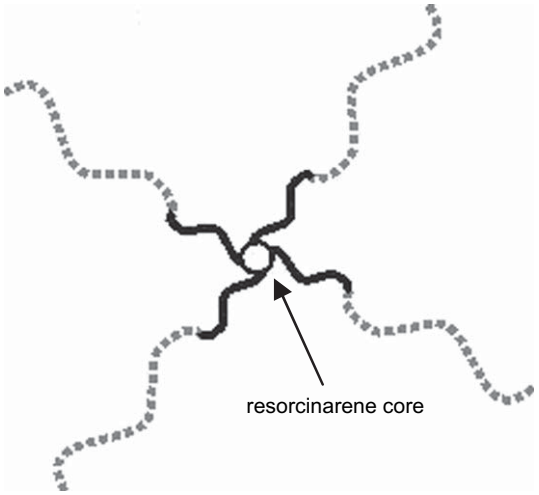


Scheme 1. Amphiphilic $(PMMA\text{-}b\text{-}PAA)_4$ star block copolymer.

organic solvents, such as THF or $CHCl_3$. The extent of hydrolysis was estimated from the $^1$H NMR spectrum of the purified polymer (Fig. 2c), being 98%. Hence, the molar mass of the final amphiphile is 71,200 g/mol when calculated from $M_n$ (SEC) and 61,300 g/mol from $M_n$ (NMR). The $M_w$ of the amphiphile was estimated using the former value and the polydispersity of the (PMMA-*b*-ptBA)$_4$ precursor given by SEC, giving $M_w$ 94,700 g/mol. Here we have assumed that the polydispersity does not change during the hydrolysis of ptBA blocks. The amphiphilic character of the polymer was demonstrated by $^1$H NMR spectroscopy: the resonance signals from PMMA core of the stars could not be seen in $D_2O$, whereas in the mixtures of acetone-$d_6$/$D_2O$ the intensities of the signals of PMMA increased upon increasing the fraction of the good solvent, acetone-$d_6$, indicating that in water the insoluble PMMA core is hidden within the uni- or multimolecular micelles formed by the (PMMA-*b*-PAA)$_4$ stars. This observation is consistent with the results of amphiphilic stars previously reported in literature [20,42].

$^1$H NMR (200 MHz, acetone-$d_6$/$D_2O$ 7:3) $\delta$ ppm: 0.81, 0.96 and 1.20 (3H, $\rangle$C(C$H_3$)−, PMMA), 1.37 (9H, −C(C$H_3$)$_3$, ptBA), 1.65 and 1.87 (6H, −C$H_2$−), 2.39 (1H, −C*H*−, PAA), 3.59 (3H, −C$H_3$, PMMA).

$^{13}$C NMR (300 MHz, acetone-$d_6$/$D_2O$ 7:3) $\delta$ ppm: 16.71 (1C, $\rangle$C(*C*H$_3$)−, PMMA), 35.07 (1C, −CH−, PAA), 41.79 (1C, −C$H_2$−, PAA), 44.61 (1C, −C$H_2$−, PMMA), 51.98 (1C, −OC$H_3$, PMMA), 54.41 (1C, $\rangle$*C*(CH$_3$)−), PMMA), 177.52 (1C, $\rangle$C═O, PMMA and 1C, $\rangle$C═O, PAA).

FT-IR (solid, ATR) cm$^{-1}$: 750 (m), 804 (m), 840 (w), 912 (w), 965 (w), 985 (w), 1060 (w), 1148 (s), 1189 (s), 1238 (s), 1366 (w), 1408 (w), 1449 (m), 1484 (w), 1547 (w), 1720 (s), 2400−3686 cm$^{-1}$ (br), 2950 (m), 2992 (w).

### 2.3. Sample preparation

Ultra high quality water purified by Elga Purelab Ultra system was used for the preparation of all solutions. The solutions were prepared by direct dissolution of the (PMMA-*b*-PAA)$_4$ in water to give 15 mg/mL, 8 mg/mL or 5 mg/mL solutions, which were equilibrated for 24 h before use. A series of concentrations for rheological studies (15−0.17 mg/mL) were obtained by consecutive dilutions. Saline solutions for light scattering and cryoTEM were prepared by the addition of concentrated NaCl (5.0 M) solution to a known volume of 5 mg/mL or 8.5 mg/mL aqueous polymer solution until the concentration of NaCl was 0.1 M. The dilutions from this solution were made using aqueous 0.1 M NaCl solution.

### 2.4. Methods

#### 2.4.1. NMR measurements

The conversions of the polymerizations and the compositions of the polymers were determined by a Varian Gemini 2000 NMR spectrometer operating at 200 MHz for $^1$H NMR and at 50.3 MHz for $^{13}$C NMR, or by a Varian UnityINOVA NMR spectrometer operating at 300 MHz for protons and 75.4 MHz for $^{13}$C. The chemical shifts are presented in parts per million downfield from the internal TMS standard or with respect to a solvent resonance line. Molar mass $M_n$ (NMR) was estimated for the (PMMA)$_4$ homopolymer by comparing the signal of the endgroup to the signals from −C$H_3$ groups, and for the (PMMA-*b*-ptBA)$_4$ by using the block ratio as well as the $M_n$ (NMR) of (PMMA)$_4$. The results are shown in Table 1.

#### 2.4.2. Size exclusion chromatography

The SEC analyses were performed with a Waters instrument equipped with a Styragel guard column, 7.8 × 300 mm Styragel capillary column and Waters 2487 UV and Waters 2410 RI detectors. THF was used as an eluent with a flow rate 0.8 mL/min. The calibration was performed with poly(methyl methacrylate) standards from PSS Polymer Standards Service GmbH.

#### 2.4.3. Rheology

The viscoelastic properties were studied with a TA Instruments AR2000 stress controlled rheometer at 20 °C. Double concentric cylinder geometry with stator inner radius of 20 mm and outer radius of 22 mm was used as measuring geometry. The volume of the sample was 7.0 mL. In order to avoid solvent evaporation from the sample the measuring chamber was covered with a lid. For the steady-shear measurements, shear rates ranging from 0.1−1000 1/s to 1000−0.1 1/s were applied. Zero-shear viscosities were calculated using TA Instruments in-built data analysis software using Cross fitting procedure:

$$\eta = \frac{\eta_0 - \eta_\infty}{1 + (\kappa\dot{\gamma})^n} + \eta_\infty, \quad (1)$$

in which $\eta_0$ is the zero-shear viscosity, $\eta_\infty$ is the viscosity at high shear, $\dot{\gamma}$ is the shear rate, $\kappa$ is the consistency index and $n$ is the slope of the curve at the inflection point. Relative viscosities $\eta_r$ were obtained by division of zero-shear viscosity of the solutions by the measured solvent viscosity. Intrinsic viscosity $[\eta]$ was determined by the extrapolation of the reduced viscosities $\eta_{red} = (\eta_r - 1)/c$ (polymer) to zero polymer concentration. For the linear viscoelastic measurements frequency sweeps were made in the linear response regime, determined by a stress sweep.

### 2.5. Light scattering

Static (SLS) and dynamic (DLS) light scattering measurements were conducted with a Brookhaven Instruments BI-200SM goniometer and a BI-9000AT digital correlator. Ar laser (LEXEL 85, $\lambda = 514.5$ nm or $\lambda = 488.0$ nm) was used as a light source. In dynamic light scattering the time autocorrelation function of scattered light intensity

$$G_2(t) = \langle I(0)I(t)\rangle \quad (2)$$

was collected in self-beating mode. The correlation function was analyzed by the inverse Laplace transform program CONTIN to obtain distributions of relaxation times, $\tau$, of corresponding correlation functions of electric field, $G_1(t)$, or distributions of hydrodynamic radii $R_h$. The values of refractive index and viscosity of water were used for the aqueous solutions. The

temperature was 20 °C and the range of studied scattering angles was 30–155°, both for dynamic and static light scatterings. The equipment was calibrated using toluene. The SLS data were treated using Zimm's double extrapolation method. The specific refractive index increments (d$n$/d$c$) of the PMMA star in THF, of the PMMA-*b*-ptBA star in toluene, and of the amphiphilic star in aqueous 0.1 M NaCl were determined at 20 °C from refractive indices measured by Billingham & Stanley Abbe60/ED refractometer using the same source of incident light. The d$n$/d$c$ for the PMMA star in THF was 0.092 mL/g ($\lambda = 514.5$ nm) [39], the d$n$/d$c$ for the PMMA-*b*-ptBA star in toluene was −0.032 mL/g ($\lambda = 488$ nm), and the d$n$/d$c$ of the amphiphilic polymer in aqueous 0.1 M NaCl was 0.157 mL/g ($\lambda = 514.5$ nm). The literature value for poly(acrylic acid) is 0.158 mL/g (0.1 M NaCl, 30 °C, $\lambda = 436$ nm) [43].

### 2.6. Cryo-electron microscopy

Aliquots (3 μL) of (PMMA-*b*-PAA)$_4$ at 5 mg/mL in water or in 0.1 M NaCl were pipetted onto 400 mesh copper grids covered with a holey carbon film (Quantifoil R 2/2) and vitrified by plunging into liquid ethane [44]. Samples were maintained at −180 °C in a Gatan 626 cryoholder whilst images were recorded on a FEI Tecnai F20 field emission gun transmission electron microscope (Electron Microscopy Unit, Institute of Biotechnology, University of Helsinki) at 200 kV under low-dose conditions at a nominal magnification of 50,000× on Kodak SO163 film. Micrographs that were free of drift and astigmatism were digitized at 7 μm intervals on a Zeiss Photoscan TD scanner resulting in a nominal sampling of 1.4 Å pixel$^{-1}$.

## 3. Results and discussion

### 3.1. Light scattering

The investigated amphiphilic star block copolymer, (PMMA-*b*-PAA)$_4$, is illustrated in Scheme 1, and the description of the amphiphile and its precursors is in Table 1, as well as in the Section 2. The (PMMA-*b*-PAA)$_4$ star dissolved well in water, but in the aqueous 0.1 M NaCl solutions (polymer concentrations $c \geq 0.015$ mg/mL) were opaque, indicating the presence of particles that are larger than in the absence of salt and that have sizes comparable to the wavelength of light. Due to the low scattering intensity, the light scattering measurements were not conducted at polymer concentrations below 0.015 mg/mL. The molar mass of these particles was measured in aqueous 0.1 M NaCl by static light scattering for the polymer concentration range 0.015–0.09 mg/mL using Zimm's double extrapolation method, which gave the weight-average molar mass $M_w = 28.6 \times 10^6$ g/mol and radius of gyration $R_g = 98$ nm. This value of molar mass corresponds to the aggregation number $N_{agg} \sim 300$, obtained by dividing the $M_w$ by the estimated $M_w$ of the amphiphile (94,700 g/mol). The aggregation number is higher than, for instance, the value reported by Burguière et al. [45] ($N_{agg} = 63$, corresponding $R_g = 67$ nm) for the aqueous $K_2CO_3$ solution of the spherical aggregates formed by an amphiphilic poly(styrene)-*block*-poly(acrylic acid) star block copolymer with 3 arms and the same block ratio, but significantly lower molar mass (5500 g/mol).

The distributions of relaxation times of $G_1(t)$ correlation functions, $\tau$, were determined by DLS for the amphiphilic star in the range of polymer concentrations ($c = 0.031$–8.53 mg/mL) in aqueous 0.1 M NaCl. Some typical relaxation time distributions obtained at 90° measuring angle are shown in Fig. 3. CONTIN algorithm is based on the Laplace inversion and is known to fail in some cases (such as broad size distributions) due to generally ill-conditioned problem of fitting the correlation functions [46]. Therefore, depending on the fitting parameters, the Laplace inversion gave either bimodal or broad monomodal distributions of relaxation times. Other origins of bimodal size distributions could be intermolecular interactions (such as aggregation, too high polymer concentrations, or the polyelectrolyte effect) or the coexistence of both rotational and translational diffusion processes typical for

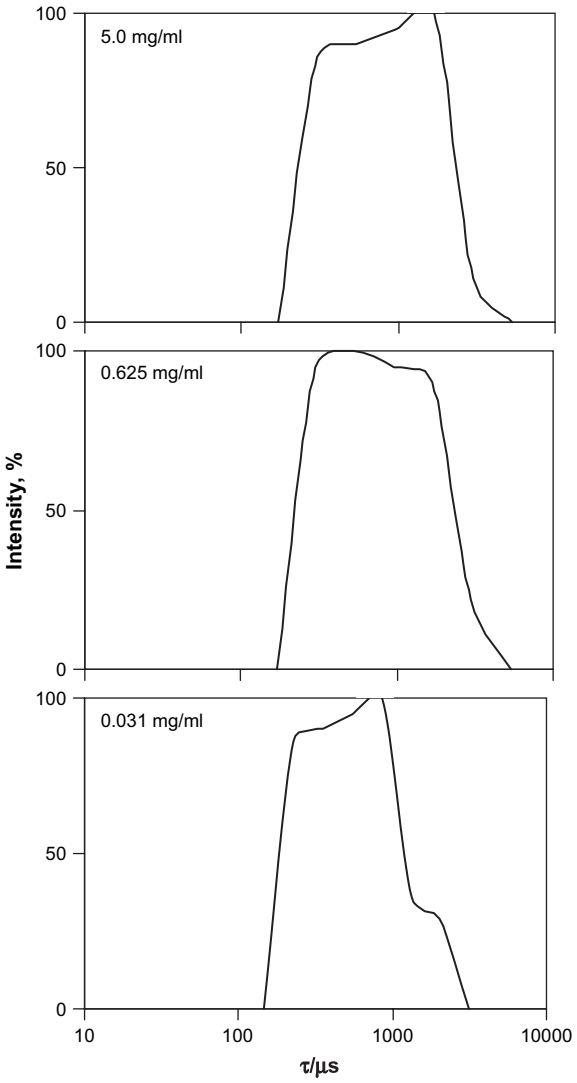


Fig. 3. Relaxation time distributions obtained at various polymer concentrations in aqueous 0.1 M NaCl at 90° scattering angle.

nonspherical species, such as rod-like micelles [47,48]. The nature of the relaxation processes was investigated for a 5 mg/mL solution through the dependence of relaxation rate $\Gamma$ on the squared amplitude of the scattering vector, $q^2$. The mean relaxation rates from the broad monomodal distributions exhibit a linear dependence on $q^2$, and the linear fit to the data passes through the origin, indicating that the relaxation times arise from translational diffusion [47].

For a 0.625 mg/mL solution, the relaxation time distribution yields the mean hydrodynamic radii $R_h$(mean) = 111 nm. However, the maximum radius, $R_{theor}$, of a single (PMMA$_{73}$-*b*-ptBA$_{143}$)$_4$ star is 54 nm, given by the contour length of an arm. As the hydrophobic core of the amphiphilic star is collapsed in aqueous solutions, the actual hydrodynamic radius of a single star is expected to be lower than $R_{theor}$. In addition, the hydrodynamic radius of the hydrophobic (PMMA-*b*-ptBA)$_4$ precursor was 7.9 nm in THF, which along with the $R_{theor}$ suggests that the $R_h$(mean) does not correspond to the hydrodynamic radius of a single amphiphilic star but rather represents intermolecular association.

There is a minor variation between the shape of the relaxation time distributions and the corresponding $R_h$(mean) within the studied range of polymer concentrations. The $R_h$(mean) decreases only slightly upon dilution. The normalized intensity autocorrelation functions of two polymer concentrations (0.25 mg/mL and 5.0 mg/mL, Fig. 4) obtained at 30° scattering angle show that the shape of the correlation function does not change considerably upon changing the polymer concentration, though the mean relaxation time shifts towards lower values. The corresponding correlation functions of the electric field in the insets of Fig. 4 clearly show the deviation from a single exponential decay due to the polydispersity of the studied samples.

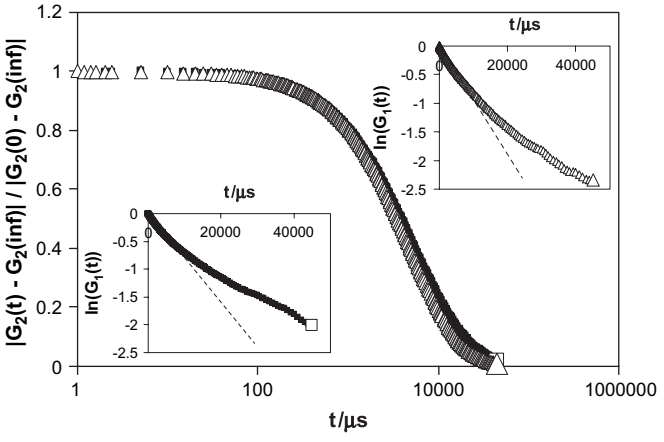


Fig. 4. Examples of normalized autocorrelation functions of the intensity of scattered light, $G_2(t)$, measured at 20 °C and 30° scattering angle. Solid square (■) corresponds to polymer concentration 5 mg/mL and open triangle (△) to 0.25 mg/mL, both in aqueous 0.1 M NaCl solution. The insets show corresponding correlation functions of electric field, $G_1(t)$, where dashed lines has been added as guide for eye and correspond to a single exponential decay. Enlarged symbols show the data points corresponding to the same delay time of the functions.

The normalized second cumulant, $(\mu_2/\Gamma^2)q^2$, is a measure of the polydispersity of the decay rate distribution and it was obtained using the second order cumulant fit:

$$\ln G_1(t) = -\Gamma t + \frac{1}{2!}\mu_2 t^2 - \frac{1}{3!}\mu_3 t^3 + \ldots \quad (3)$$

$\Gamma = \tau^{-1}$ is the decay rate also called the first cumulant, $\mu_2$ and $\mu_3$ are the second and third cumulants, $q = (4\pi n_0/\lambda_0)\sin(\theta/2)$ is the amplitude of the scattering vector, $n_0$ is the refractive index of the solvent, $\lambda_0$ is the wavelength in vacuum, and $\theta$ is the scattering angle. The inset in Fig. 5 shows that the normalized second cumulant extrapolated to 0° scattering angle is nearly constant and its average value of 0.27 is typical for polydisperse samples. This, along with the relaxation time distributions, refers to the stability of the aggregates: once the aggregates are formed, the system seems to be rather stable towards dilution by aqueous 0.1 M NaCl solution. The stability of the aggregates was confirmed by the fact that no significant changes in the size distributions were observed during 6 weeks storage in a refrigerator or upon gradual heating of the solution to 50 °C within 4 h.

The most expected conformation of supramolecular aggregates of amphiphilic star-like polymers is a sphere [35]. Fig. 5 depicts the angular dependence of the average values of the diffusion coefficient $D_\theta = \Gamma/q^2$. As the diffusion coefficient of the monodisperse spherical species, such as micelles, has no angular dependence, our results indicate that the dependence originates either from polydispersity of the studied aggregates or from their nonspherical shape. The angular dependence of the diffusion coefficients was observed within the whole range of studied polymer concentrations in aqueous 0.1 M NaCl solution.

The radius of gyration $R_g$ of the amphiphile was calculated for 5 mg/mL and 1.25 mg/mL aqueous solutions in 0.1 M NaCl from the linear region of the particle scattering function,

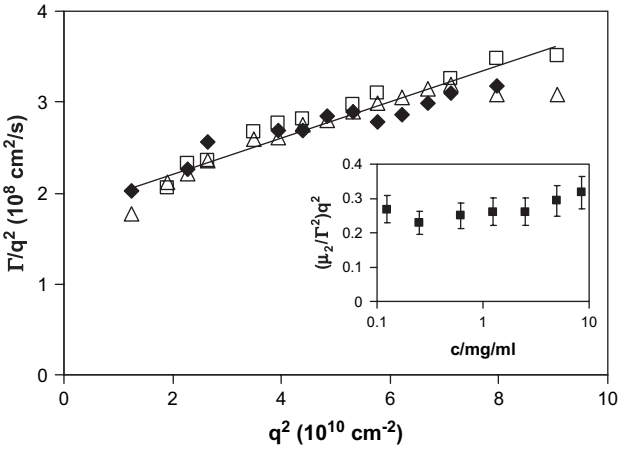


Fig. 5. The diffusion coefficients $\Gamma/q^2 = D_\theta$ as a function of $q^2$ for 0.25 mg/mL (open triangles), 1.25 mg/mL (open squares), and 5 mg/mL (solid diamonds) polymer solutions at 0.1 M NaCl. The values of $\Gamma$ have been obtained by second order cumulant fit. The inset depicts the values of normalized second cumulant, $(\mu_2/\Gamma^2)q^2$, representing the polydispersity of the decay rate distribution at 0° scattering angle, as a function of polymer concentration.

$P(q) = R_\theta/R_{\theta=0}$, which gave the values of $R_g$=127.9 nm and 162.5 nm, respectively. Fig. 6 shows Kratky representation $(qR_g)^2P(q)$ versus $qR_g$ for solutions of the same polymer concentrations. At low values of $qR_g$ the particles resemble a common random coil as they are seen in the scattering experiment comprising a large number of Kuhn segments, and therefore, theoretical particle scattering functions shown in Fig. 6 coincide [49,50]. At large values of $qR_g$ ($qR_g > 2$) shorter sections of the particles are probed and the structure of the particles can be revealed by the Kratky plot, in which the asymptotic part is strongly amplified making the differences in structure distinguishable. Thus, for star-like polymers with the low number of arms a model of a random coil may still be valid, whereas increasing the number of arms leads to the Debye–Bueche behavior typically describing branched structures [51,52]. The experimental data obtained from the 5 mg/mL solutions of the amphiphilic stars in the $qR_g > 2$ region coincide well with the theoretical predictions representing either polydisperse rods [53] or worm-like chains [54,55]. The difference between the curves of two polymer concentrations may arise from the polydispersity of the structures formed in the 1.25 mg/mL solution. For more precise conformation analysis one needs either other scattering techniques providing larger $q$-values (X-rays or neutrons) or other research methods. In this study we employed electron microscopy (see below) in order to visualize the structures formed in the same 5 and 1.25 mg/mL solutions, and thus verify the conclusions from the light scattering data.

The ratio of the radius of gyration, $R_g$ and the hydrodynamic radius, $R_h$, $R_g/R_h$, has frequently been used to describe the structure of the species in solution. $R_g/R_h$(mean) is 1.54 for the 5 mg/mL solution of the amphiphile and 1.50 for the 1.25 mg/mL solution. The literature value of $R_g/R_h$ for rigid rods is >2.0, both for mono- and polydisperse systems and hence, the values of $R_g/R_h$(mean) would rather refer to random coils (literature values of $R_g/R_h = 1.50$ for monodisperse and 2.05 for polydisperse systems in good solvent) or regular stars (literature value for $R_g/R_h = 1.33$ for a 4-arm star in $\theta$ solvent) than rigid rods [56]. However, one must bear in mind that the relaxation time distributions indicate a polydisperse system, and if there are various types of aggregates present in the solution, the values of $R_g/R_h$ may not be applied.

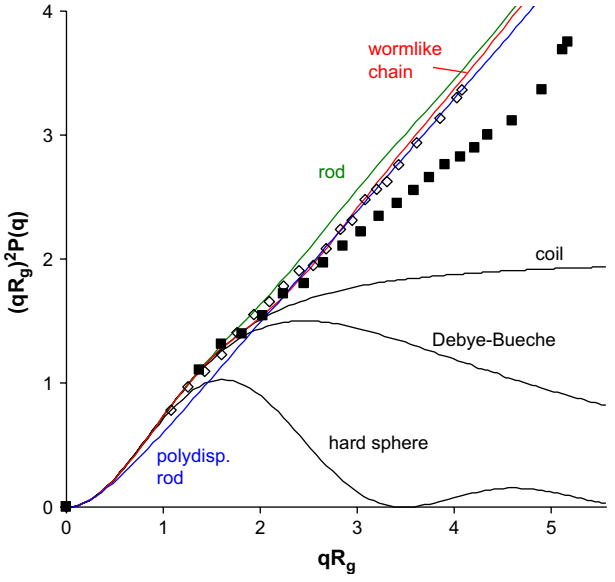


Fig. 6. Kratky representation $(qR_g)^2P(q)$ versus $qR_g$ of the experimental particle scattering functions, $P(q) = R_\theta/R_{\theta=0}$, for 5 mg/mL (open symbols) and 1.25 mg/mL (solid symbols) solutions of the amphiphilic stars. Theoretical curves for model macromolecular structures have been added for comparison as solid lines.

### 3.2. Viscoelastic behavior of salt-free aqueous solutions

The rheological behavior is dependent on the structure of the species in solution and thus, the interactions between the amphiphilic stars, or rather between their aggregates as indicated by the cloudiness of the aqueous solutions, were investigated by the rheological methods in the absence of salt. The addition of salt (0.1 M NaCl) reduced the viscosities of the solutions close to that of the solvent and resulted in shear induced precipitation due to decreased electrosteric stabilisation of the aggregates having a polyelectrolyte shell. This solution behavior resembles the one described by Korobko et al. [28] for strongly interacting micelles of linear poly(acrylic acid)-*block*-poly(styrene) that has interpenetrated polyelectrolyte coronal layers, which could be an additional reason for the precipitation of the studied star polymers at high polymer concentrations. Because of the precipitation, rheological investigations were not conducted in the presence of salt. The viscosity curves of some of the aqueous polymer solutions are depicted in Fig. 7. The solutions with low polymer concentrations (≤1.6 mg/mL) exhibited Newtonian flow throughout the studied shear rates, whereas shear thinning was observed at higher polymer concentrations (2–15 mg/mL). The onset of shear thinning was around shear rate 40–80 1/s, shifting to lower shear rates with increasing concentration. There was no significant hysteresis in the flow curves during subsequent experiments, suggesting that the structure of the solution does not change irreversibly during the measurements.

The analysis of the flow curves by Cross fitting procedure (Eq. (1)) gave zero-shear viscosities, which yield the relative viscosity $\eta_{rel} = \eta_0/\eta_s$ when divided by solvent viscosity $\eta_s$. The critical overlap concentration $c^*$ of the salt-free solutions was calculated from the intrinsic viscosity $[\eta]$ of the dilute regime ($c^* = [\eta]^{-1}$), which gave $c^* = 1.7$ mg/mL. The strong increase in the relative viscosities above the concentration $c^*$ where the aggregates of the polymers start to overlap, in the present case at 1.7 mg/mL (inset in Fig. 8), is typical for micellar systems [25]. The $c^*$ in a saline solution could not be measured by this technique but it may be assumed to be somewhat higher than in pure water due to lower viscosities of the solutions.

The concentration dependence of $\eta_{rel}$ above the $c^*$ reflects the "softness" of colloidal systems, since the zero-shear viscosity of hard-sphere systems diverges at the maximum packing fraction while for polymer-like samples a lower scaling factor is expected. In the present case the viscosity of the

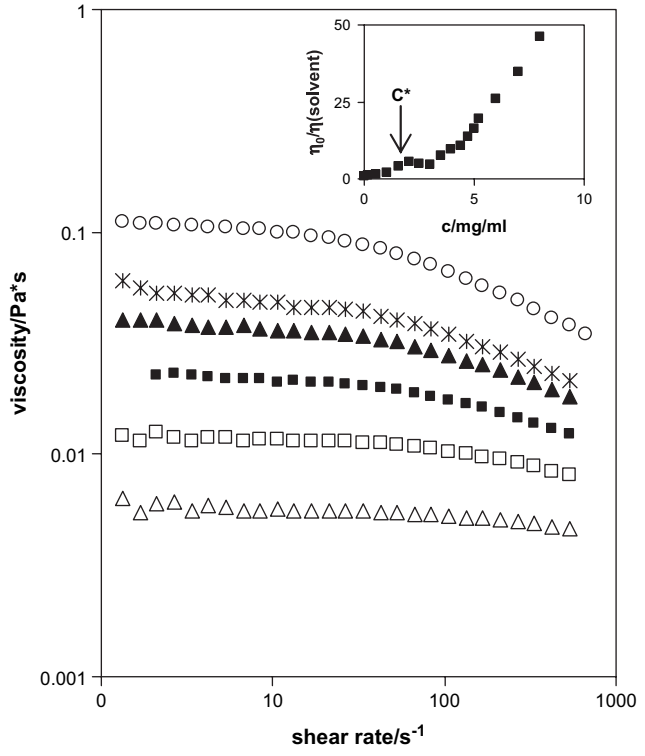


Fig. 7. Flow curves of the amphiphile in distilled water at different concentrations: (○) 15 mg/mL, (✳) 8.0 mg/mL, (▲) 7.0 mg/mL, (■) 5.0 mg/mL, (□) 3.9 mg/mL, and (△) 3.0 mg/mL. The inset shows the relative viscosity against the concentration of the amphiphile.

aggregated stars above the $c^*$ scales up approximately as $\eta_{rel} \propto c^{2.5}$, which is the theoretical scaling of linear polymers above $c^*$ [21,57]. The weak shear thinning behavior and the observed concentration dependence indicate that the star polymers do not behave as hard spheres and they do not form an interconnected network at the studied concentration range.

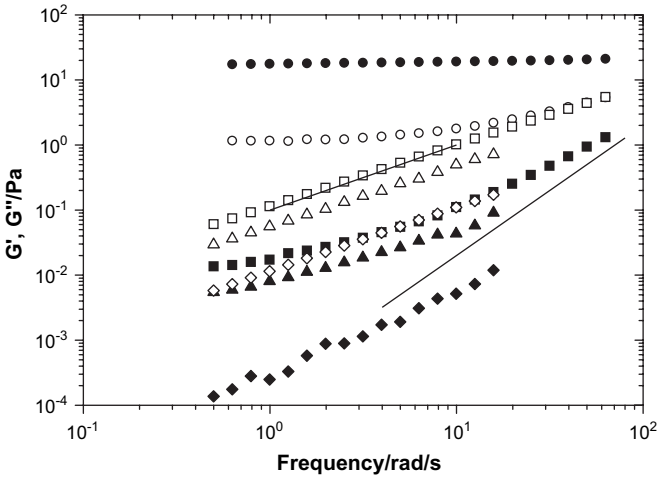


Fig. 8. Storage and loss moduli versus frequency of the amphiphile at concentration of 15 mg/mL (■,□), 8.0 mg/mL (▲,△) and 3.9 mg/mL (◆,◇) in water directly after flow measurement and of 15 mg/mL (● ○) after 14 h waiting. Filled symbols are for $G'$ and open symbols for $G''$. The straight lines show theoretical scaling of the moduli as $G'$ scales up $\sim\omega^1$ and $G''$ $\sim\omega^2$.

The amphiphilic star shows striking time-dependent viscoelastic properties in a semidilute solution (15 mg/mL). Fig. 8 shows the frequency dependencies of the storage ($G'$) and loss ($G''$) moduli for various polymer concentrations. The samples presheared in a flow measurement with a maximum shear rate of 1000 1/s behave as a viscous liquid as $G''$ exceeds $G'$ throughout the studied frequency range. The moduli for the 15 mg/mL presheared sample scale with frequency as it is typical for viscoelastic Maxwellian fluids, that is, $G''$ scales with $\omega^2$ and $G'$ with $\omega^1$. However, after the 15 mg/mL sample was allowed to stand undisturbed in the measuring cylinder, the elastic modulus built up slowly and after 14 h the sample reached a soft gel-like behavior with $G' > G''$ over the entire studied frequency range. The fluid-like character reappeared upon shearing the gel. The slow gelation may stem from the formation of a physical network owing to hydrophobic interactions or to the interpenetration of the coronal layers. Due to the repulsion between the PAA chains in the absence of the salt, the association between the micelles can be easily broken after which the sample exhibits fluid-like character.

It has been reported that elongated or worm-like micelles exhibit gel-like behavior at higher concentrations [48]. The gelation of star-shaped colloids typically takes place at high polymer concentrations due to an order–disorder transition near the close packing volume fraction [58]. This transition is dependent on concentration, on the composition of the stars and on temperature [59,60]. Hence, in addition to the hydrophobic association, the gelation of the amphiphilic stars or their micelles could occur upon the interpenetration of the soft coronas resulting in the entanglement of the PAA blocks, as described by Korobko et al. [28] for micellar systems of linear polyelectrolyte block copolymers. High molar mass, low number of arms and star-like architecture have been observed to favor gelation of neutral block copolymers: for example with block copolymers of poly(L-lactide) and poly(ethylene oxide) the gelation in aqueous solutions has been observed to occur at lower polymer concentration by star polymers than by linear analogues with the same poly(ethylene oxide) content [60]. Park et al. have also reported that the gelation due to hydrophobic association of amphiphilic stars is dependent on the fraction of the hydrophobe in the polymer [60].

### 3.3. Cryo-electron microscopy

Two major classes of particles are seen in cryo-electron micrographs (Fig. 9) of a 5 mg/mL solution of the star-like amphiphile in aqueous 0.1 M NaCl. Small spherical micelle-like aggregates [61] with visible radiating arms can be observed, as well as flexible worm-like aggregates of varying lengths. The worm-like species are also rough at the edges, with similar radiating arms as in the spherical micelles. According to the micrographs the diameter of the spherical micelles is $19 \pm 3$ nm, being also the approximate diameter of the worm-like micelles. The length of the worm-like micelles is $195 \pm 25$ nm.

The electron micrograph of the saline solution of the amphiphile verifies the light scattering results in the presence

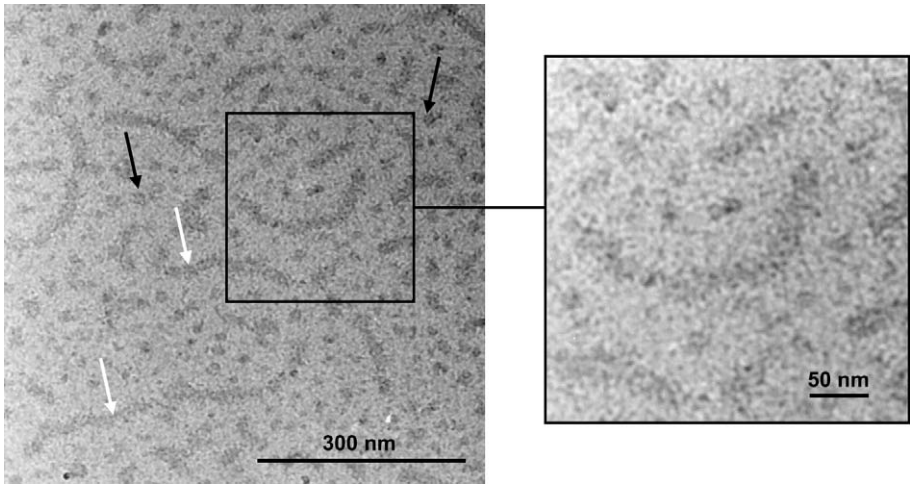


Fig. 9. Representative cryo-electron micrographs of (PMMA-*b*-PAA)$_4$ star polymer in 5 mg/mL aqueous 0.1 M NaCl solution (underfocus 8.4 μm). The black arrows point to spherical micelles and the white arrows to the worm-like ones. Inset shows an enlargement of micelles displaying radiating arms.

of nonspherical micelle-like aggregates. Comparison of cryo-TEM images with the Kratky presentation (Fig. 6) shows that the scattering from the 5 mg/mL solution is primarily determined by the large worm-like species. The 1.25 mg/mL solution may either contain highly polydisperse worm-like chains or larger relative number of spherical aggregates than in the more concentrated solution. In addition, light scattering emphasizes large scatterers in solution and hence the scattering from smaller spherical micelles is engulfed. This is the case for 1.25 mg/mL solution, for which DLS fails to resolve the composition. As a result, the size distribution for 1.25 mg/mL solution is apparently monomodal and broad and $R_h$(mean) is smaller than that in 5 mg/mL solution.

The small discrepancies in the size of the worm-like micelles determined from DLS and from the cryoTEM images evidently originate from the difference in contrast between the compact PMMA core of the micelles and the less dense shell of the hydrophilic PAA blocks, the latter is seen as roughness or 'fuzziness' in the micellar species, which makes it difficult to estimate the confines of the micelles.

The large molar mass of the block copolymer given by SLS (Table 1) suggests that some star–star coupling has occurred during the synthesis. The presence of coupled stars in the aggregates could broaden their size distributions, thus making the determination of the particle sizes more complicated.

The cryoTEM image of a salt-free aqueous 5 mg/mL solution of the amphiphile (Fig. 10) shows the coexistence of spherical micelles and micellar species that could rather be described as elongated or clustered, than wormlike. Obviously, screening of electrostatic interactions by the addition of salt plays an important role in the formation of worm-like species. Crowding of the micelles at the thicker edges of the biconcave cryoTEM sample is known to occur during sample preparation due to size segregation of the particles in solution [62,63]. This is unlikely to be the reason for the formation of worm-like species as these are observed also in the thinner parts in the middle of the sample.

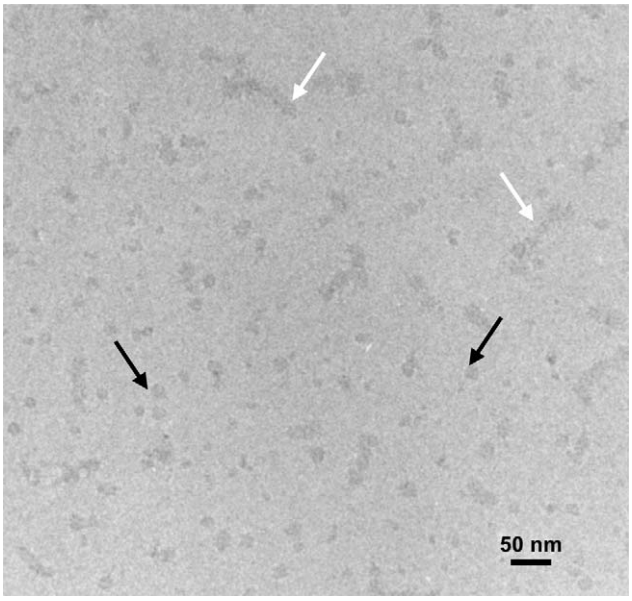


Fig. 10. Representative cryo-electron micrograph of (PMMA-*b*-PAA)$_4$ star polymer in 5 mg/mL salt-free aqueous solution (underfocus 6.8 μm). The black arrows point to spherical micelles and the white arrows to the elongated ones.

## 4. Conclusions

Water-soluble 4-armed star amphiphiles with a PMMA core and a PAA corona show a tendency to associate in aqueous solutions. Like their linear analogues, amphiphilic star-like block copolymers tend to diminish the exposure of the hydrophobic blocks to water, and thus aggregate into micelles. Burguière et al. [45] have suggested that the star block copolymers form micelles in a similar way as linear diblock copolymers, that is, the aggregation number $N_{agg}$ of the micelles is strongly dependent on the lengths of the hydrophilic and hydrophobic blocks and the micellization is controlled by the interchain distance between the hydrophilic blocks in corona. According to Huh and coworkers [35] the

micellization makes the stars to adopt restricted conformations in the spherical geometry, thus giving rise to a loss in conformational entropy.

According to Zhang and Eisenberg [1], the formation of different micellar morphologies in the aqueous solutions of amphiphilic block copolymers is governed by the extension of the hydrophobic blocks in the micellar core, the surface tension between the core and the solvent, and the repulsion between the hydrophilic chains in the corona. In case the hydrophilic block is ionic, like poly(acrylic acid), the balance between these factors can be perturbed by the addition of salt which decreases the electrostatic repulsion in the corona, favoring a further aggregation of the amphiphiles and thus increasing the aggregation number [64,65]. We observed that the addition of salt induced the formation of worm-like micelles of the amphiphilic star block copolymers, and spherical and worm-like micelles coexisted within the studied concentration range. This is in accordance with the observations from the linear amphiphiles with charged hydrophilic blocks [66,67]. Increasing the aggregate size is thermodynamically favorable in order to reduce the interfacial area between the solvent and the hydrophobic core [1,9]. Further aggregation would lead to an increase in the radius of the core and stretching of the chains. Hence, according to Zhang and Eisenberg [1], an additional degree of freedom could be attained without significant changes in conformation by changing the micellar morphology from spherical to cylindrical. Other factors that may affect the micellization process include temperature, ionic strength and pH of the solvent, and these will be subject of further studies. The interaction between the micelles of the amphiphilic stars was observed as the shear thinning behavior of the salt-free polymer solutions as well as in their tendency to form gels at semidilute polymer concentrations due to both the hydrophobic association and the softness of the corona.

The formation of cylindrical or worm-like polymer micelles by linear amphiphilic block copolymers with different compositions and block ratios has been observed earlier [1,3,17], as well as that by amphiphilic miktoarm star copolymers, in which the arms rearrange to separate hydrophobic and hydrophilic domains to induce aggregation [36]. Amphiphilic star block copolymers have been treated as representatives of unimolecular micelles in dilute solutions [20], but according to the evidence above, when the number of arms is low they are also capable of forming multimolecular assemblies like spherical or worm-like micelles or both, depending on the polymer concentration and the solvent condition. These assemblies mimic the ones formed by globular cytoskeletal proteins such as tubulin or actin, which contain acidic groups to provide polyelectrolyte nature. For instance, in laboratory conditions G-actin forms filamentous F-actin upon addition of salt [37]. Recently, a report has been published on applications of worm-like micelles as drug delivery vehicles resembling natural filamentous phages, which have significantly longer circulation times *in vivo* than spherical carriers [68]. Other possible applications could include unimolecular and self-assembled nanoreactors [69].

## Acknowledgements

The authors gratefully acknowledge Professor R. Serimaa for her help in LS data interpretation, and for financial support by ESPOM Graduate School (Electrochemical Science and Technology of Polymers and Membranes including Biomembranes). Sarah J. Butcher is an Academy of Finland fellow. The authors also wish to thank Professor W. Burchard for helpful discussions.

## References

[1] Zhang L, Eisenberg A. J Am Chem Soc 1996;118:3168–81.
[2] Discher DE, Eisenberg A. Science 2002;297:967–73.
[3] Geng Y, Ahmed F, Bhasin N, Discher DE. J Phys Chem B 2005; 109:3772–9.
[4] Li Z, Kesselman E, Talmon Y, Hillmyer MA, Lodge TP. Science 2004; 306:98–101.
[5] Pochan DJ, Chen Z, Cui H, Hales K, Qi K, Wooley KL. Science 2004; 306:94–7.
[6] Cornelissen J, Fischer M, Sommerdijk N, Nolte RJM. Science 1998; 280:1427–30.
[7] Whitesides GM, Simanek EE, Mathias JP, Seto CT, Chin DN, Mammen MM, et al. Acc Chem Res 1995;28:37–44.
[8] Choucair A, Lavigueur C, Eisenberg A. Langmuir 2004;20:3894–900.
[9] Zhang L, Eisenberg A. Macromolecules 1999;32:2239–49.
[10] Ma Q, Remsen EE, Clark Jr CG, Kowalewski T, Wooley KL. Proc Natl Acad Sci USA 2002;99:5058–63.
[11] Dalhaimer P, Engler AJ, Parthasarathy R, Discher DE. Biomacromolecules 2004;5:1714–9.
[12] Spatz JP, Herzog T, Mössmer S, Ziemann P, Möller M. Adv Mater 1999; 11:149–53.
[13] Boontongkong Y, Cohen RE. Macromolecules 2002;35:3647–52.
[14] Burke SE, Eisenberg A. Langmuir 2001;17:6705–14.
[15] Borisov OV, Zhulina EB. Langmuir 2005;21:3229–31.
[16] Ma Q, Wooley K. J Polym Sci Part A Polym Chem 2000;38:4805–20.
[17] Dalhaimer P, Bates FS, Discher DE. Macromolecules 2003;36:6873–7.
[18] Joralemon MJ, O'Reilly RK, Hawker CJ, Wooley KL. J Am Chem Soc 2005;127:16892–9.
[19] Guo X, Ballauff M. Langmuir 2000;16:8719–26.
[20] Heise A, Hedrick JL, Frank CW, Miller RD. J Am Chem Soc 1999; 121:8647–8.
[21] Vlassopoulos D, Fytas G, Pispas S, Hadjichristidis N. Physica B 2001; 296:184–9.
[22] Semenov AN, Vlassopoulos D, Fytas G, Vlachos G, Fleischer G, Roovers J. Langmuir 1999;15:358–68.
[23] Senff H, Richtering W, Norhausen Ch, Weiss A, Ballauff M. Langmuir 1999;15:102–6.
[24] Furukawa T, Ishizu K. Macromolecules 2005;38:2911–7.
[25] Buitenhuis J, Förster S. J Chem Phys 1997;107:262–72.
[26] Bhatia SR, Mourchid A, Joanicot M. Curr Opin Colloid Interface Sci 2001;6:471–8.
[27] Tan BH, Kam KC, Lam YC, Tan CB. Polymer 2004;45:5515–23.
[28] Korobko AV, Jesse W, Lapp A, Egelhaaf SU, van der Maarel JRC. J Chem Phys 2005;122:024902.
[29] Vlassopoulos D. J Polym Sci Part B Polym Phys 2004;42:2931–41.
[30] Gitsov I, Fréchet JMJ. J Am Chem Soc 1996;118:3785–6.
[31] Yoo M, Heise A, Hedrick JL, Miller RD, Frank CW. Macromolecules 2003;36:268–71.
[32] Chen X, Smid J. Langmuir 1996;12:2207–13.
[33] Narrainen AP, Pasqual S, Haddleton DM. J Polym Sci Part A Polym Chem 2002;40:439–50.
[34] Kim KH, Cui GH, Lim HJ, Huh J, Ahn CH, Jo WH. Macromol Chem Phys 2004;205:1684–92.
[35] Huh J, Kim KH, Ahn CH, Jo WH. J Chem Phys 2004;121:4998–5004.

[36] Teng J, Zubarev ER. J Am Chem Soc 2003;125:11840–1.
[37] Tang JX, Janmey PA. J Biol Chem 1996;271:8556–63.
[38] Nikitine S, Heimburger R, Ringeissen J, Schwab C. Pat. Appl. 1968; FR 1523459.
[39] Strandman S, Luostarinen M, Niemelä S, Rissanen K, Tenhu H. J Polym Sci Part A Polym Chem 2004;42:4189–201.
[40] Strandman S, Pulkkinen P, Tenhu H. J Polym Sci Part A Polym Chem 2005;43:3349–58.
[41] Angot S, Murthy KS, Taton D, Gnanou Y. Macromolecules 2000;33: 7261–74.
[42] Matmour R, Raju F, Duran RS, Gnanou Y. Macromolecules 2005;38: 7754–67.
[43] Brandrup J, Immergut EH, Grulke EA, editors. Polymer handbook. 4th ed. New York, Chichester, Weinheim, Brisbane, Singapore, Toronto: John Wiley & Sons, Inc.; 1999. p. VII/547.
[44] Adrian M, Dubochet J, Lepault J, McDowall AW. Nature 1984;308:32–6.
[45] Burguière C, Chassenieux C, Charleux B. Polymer 2003;44:509–18.
[46] Peters R. In: Brown W, editor. Dynamic light scattering: the method and some applications. Oxford: Clarendon Press; 1993. p. 149.
[47] Schillén K, Brown W, Johnsen RM. Macromolecules 1994;27:4825–32.
[48] Jørgensen EB, Hvidt S, Brown W, Schillén K. Macromolecules 1997;30: 2355–64.
[49] Kratochvil P. In: Huglin MB, editor. Light scattering from polymer solutions. London: Academic Press; 1972. p. 333.
[50] Pedersen JS. Adv Colloid Interface Sci 1997;70:171–210.
[51] Savin G, Burchard W. Macromolecules 2004;37:3005–17.
[52] Burchard W. Macromolecules 2004;37:3841–9.
[53] Goldstein M. J Chem Phys 1953;21:1255–8.
[54] Yoshizaki T, Yamakawa H. Macromolecules 1980;13:1518–25.
[55] Pedersen JS, Schurtenberger P. Macromolecules 1996;29:7602–12.
[56] Burchard W. In: Harding SE, Sattelle DB, Bloomfield VA, editors. Laser light scattering in biochemistry. Cambridge: Royal Society of Chemistry; 1992. p. 11.
[57] Kjøniksen A-L, Laukkanen A, Galant C, Knudsen KD, Tenhu H, Nyström B. Macromolecules 2005;38:948–60.
[58] Castaing J-C, Allain C, Auroy P, Auvray L. Eur Phys J B 1999; 10:61–70.
[59] Loppinet B, Stiakakis E, Vlassopoulos D, Fytas G, Roovers J. Macromolecules 2001;34:8216–23.
[60] Park SY, Han BR, Na KM, Han DK, Kim SC. Macromolecules 2003; 36:4115–24.
[61] As the PMMA core of the assemblies is below the $T_g$, these nonequilibrium structures should be called 'micelle-like aggregates'. However, the term 'micelle' is extensively used in literature and hence, we will use it here.
[62] Dubochet J, Adrian M, Chang J-J, Homo J-C, Lepault J, McDowall AW, et al. Quart Rev Biophys 1988;21:129–228.
[63] Talmon Y. Ber Bunsen-Ges Phys Chem 1996;100:364–72.
[64] Antoun S, Gohy J-F, Jérôme R. Polymer 2001;42:3641–8.
[65] Pergushov DV, Remizova EV, Gradzielski M, Lindner P, Feldthusen J, Zezin AB, et al. Polymer 2004;45:367–78.
[66] Zhang L, Eisenberg A. Macromolecules 1996;29:8805–15.
[67] Förster S, Abetz V, Müller A. Adv Polym Sci 2004;166:173–210.
[68] Geng Y, Discher D. Polym Prepr 2005;46:176–7.
[69] Vriezema DM, Aragonès MC, Elemans JAA, Cornelissen JJL, Rowan AE, Nolte RJM. Chem Rev 2005;105:1445–90.